forensic sciences

MDPI

Article

Rethinking the Postmortem Pupil: Biological Insights Through the Standardization of Miosis and Mydriasis

Matteo Nioi [1,*], Pietro Emanuele Napoli [2], Djordje Alempijevic [3], Aleksandar Stankov [4], Domenico Nieddu [1], Alberto Chighine [1], Emanuela Locci [1] and Ernesto d'Aloja [1]

[1] Forensic Medicine Unit, Department of Medical Sciences and Public Health, University of Cagliari, 09040 Cagliari, Sardinia, Italy; nieddu_domenico@hotmail.it (D.N.); alberto.chighine@unica.it (A.C.); elocci@unica.it (E.L.); ernesto.daloja@unica.it (E.d.)
[2] Studio Oculistico Dr. Pietro Emanuele Napoli, 09014 Carloforte, Sardinia, Italy; pietronapoli@ymail.com
[3] Faculty of Medicine, Institute of Forensic Medicine, University of Belgrade, 11000 Belgrade, Serbia; djordje.alempijevic@med.bg.ac.rs
[4] Institute for Forensic Medicine, Ss. Cyril & Methodius University, 1000 Skopje, North Macedonia; astankov@medf.ukim.edu.mk
* Correspondence: nioimatteo@gmail.com; Tel.: +39-349-086-8477

Abstract

Background/Objectives: Postmortem pupillary assessment remains qualitative and lacks standardized quantitative criteria. The Pupil-to-Iris Ratio (PIR), a described photographic morphometric measure, enables objective postmortem pupil characterization independent of image magnification. This study aimed to establish a standardized PIR framework, characterize baseline postmortem pupillary morphology, and investigate its biological determinants. **Methods:** Retrospective study of 83 forensic cases (166 eyes) with postmortem intervals of 3–288 h. Digital photographs were analyzed using a semi-automated workflow. A predefined proposed operational PIR classification was applied. Associations with age, sex, postmortem interval, cause of death, and toxicology were evaluated using mixed-effects models and generalized estimating equations. **Results:** Quantitative PIR assessment was successful in all eyes. Neutral morphology predominated (119/166 eyes, 71.7%), while miotic and mydriatic phenotypes, including their extreme categories, accounted for 17/166 (10.2%) and 30/166 eyes (18.1%), respectively. Age showed a significant inverse association ($\rho = -0.352$, $p = 0.001$). Toxicological analyses showed poor discriminatory performance (direction-normalized AUCs, defined as max [AUC, 1 − AUC], of 0.553–0.606). Intra-observer repeatability across a randomly selected subset of 62 eyes was excellent (ICC(2, 1) = 0.919), with no statistically significant systematic difference between the two measurement sessions ($p = 0.052$). **Conclusions:** Standardized PIR assessment provides an objective framework for postmortem pupillary characterization. This study establishes a reproducible methodological foundation for future postmortem pupillometry research.

Keywords: Pupil-to-Iris Ratio (PIR); postmortem pupil; postmortem pupillary morphology; quantitative pupillary morphometry; forensic medicine; forensic pathology; postmortem examination; miosis and mydriasis definition; miosis and mydriasis classification; digital morphometry

Check for updates

Academic Editors: Ricardo Jorge Dinis-Oliveira and Sorin Hostiuc

Received: 13 July 2026
Revised: 9 August 2026
Accepted: 9 October 2026
Published: 13 October 2026

Copyright: © 2026 by the authors. Licensee MDPI, Basel, Switzerland. This article is an open access article distributed under the terms and conditions of the Creative Commons Attribution (CC BY) license.

1. Introduction

The pupil is a dynamic ocular structure whose diameter reflects the continuous interaction between the sympathetic and parasympathetic nervous systems. Beyond regulating

retinal illumination, pupillary size is influenced by physiological variables, neurological disorders, systemic diseases, medications, and psychoactive substances, making it an important clinical biomarker in ophthalmology, neurology, and toxicology [1–4]. Quantitative assessment of pupillary function has therefore become an integral component of neurological examination and automated pupillometry is increasingly used to support clinical decision-making. Under physiological conditions, pupil size varies according to multiple intrinsic and extrinsic factors, including ambient illumination, accommodation, age, circadian rhythm, cognitive state, and individual autonomic balance. Among these variables, ageing is the most consistently documented determinant, with resting pupil diameter gradually decreasing after early adulthood because of structural and functional changes affecting the iris and its autonomic innervation [5,6]. In addition, numerous medications, systemic diseases, and environmental exposures may alter pupillary morphology through direct pharmacological effects or autonomic dysfunction. Ophthalmic drugs, nicotine, alcohol consumption, and diabetes mellitus are well-recognized examples that should be considered when interpreting pupillary findings [7–12]. Pupillary abnormalities also represent valuable indicators of neurological and toxicological conditions. In patients with traumatic brain injury, alterations in pupil size and reactivity provide important information regarding brainstem function and intracranial pathology, while automated infrared pupillometry has substantially improved the objectivity and reproducibility of these measurements [13–17]. Likewise, drugs of abuse produce characteristic autonomic responses involving the pupil. Opioids typically induce miosis, sympathomimetic stimulants such as cocaine and amphetamines cause mydriasis, whereas cannabis produces more variable effects depending on dose, timing, and individual susceptibility. Although these responses are routinely considered during clinical and forensic toxicological assessment, their interpretation remains influenced by multiple premortem variables, including pharmacological tolerance, concomitant drug exposure, and environmental conditions [18–25].

1.1. Postmortem Pupillary Changes

Following somatic death, the physiological regulation of the pupil ceases because of the irreversible loss of central nervous system activity and autonomic control. Consequently, the pupillary light reflex disappears and the pupil becomes fixed. During routine forensic examination, pupillary morphology is systematically documented as part of the external inspection of the body. However, current descriptions remain largely qualitative, and standardized quantitative criteria for defining postmortem miosis, mydriasis, or intermediate pupillary configurations are not available [26,27]. Despite the loss of neural regulation, the iris temporarily retains residual cellular viability, allowing transient pharmacological responses during the early postmortem interval. This phenomenon, known as postmortem chemical iris excitability, has been investigated for more than a century as a potential method for estimating the postmortem interval [28,29]. Nevertheless, subsequent studies demonstrated considerable inter-individual variability, inconsistent pharmacological responses, and poor reproducibility, leading to the current consensus that pharmacological iris testing cannot be considered a reliable standalone tool for postmortem interval estimation [30–32]. Beyond pharmacological stimulation, spontaneous postmortem changes in pupil size have also been investigated. Although several studies have reported progressive constriction, secondary dilation, or other temporal patterns, their findings remain inconsistent and no reproducible chronological evolution has been demonstrated. More recently, digital image analysis has shown excellent reliability for measuring the pupil-to-iris relationship, yet available evidence still does not support the existence of a uniform postmortem pupillary state or standardized quantitative criteria suitable for routine forensic practice [33,34]. At the same time, forensic ophthalmology has

undergone substantial development through the introduction of objective ocular imaging techniques. Optical coherence tomography and other imaging approaches have enabled detailed characterization of postmortem changes involving the cornea, anterior chamber, sclera, and other ocular structures, demonstrating that the eye undergoes a coordinated process of postmortem transformation rather than isolated morphological alterations [35–38]. In contrast, quantitative evaluation of postmortem pupillary morphology has advanced only marginally and continues to rely predominantly on descriptive observations. This discrepancy highlights the need for standardized morphometric methods capable of providing objective, reproducible, and comparable measurements of the postmortem pupil.

1.2. Rationale and Objectives of the Study

Although the postmortem pupil has been investigated for decades, its forensic evaluation remains largely qualitative, and standardized quantitative criteria for describing pupillary morphology are still lacking. Previous studies have primarily focused on pharmacological iris reactivity or absolute pupil diameter, yielding heterogeneous findings that have limited comparisons across studies and prevented the development of reproducible approaches suitable for routine forensic practice [30–34].

Recent advances in forensic ophthalmology and computer-assisted image analysis have enabled increasingly objective assessment of postmortem ocular structures [35–37]. However, unlike corneal and scleral changes, postmortem pupillary morphology has not yet been investigated using a standardized morphometric framework.

The aim of this study was to establish a standardized quantitative framework for postmortem pupillary assessment based on the Pupil-to-Iris Ratio (PIR), characterize baseline postmortem pupillary morphology, and investigate its principal biological determinants in a forensic population. We hypothesized that PIR would provide a reproducible morphometric descriptor for the objective classification of postmortem pupillary morphology and facilitate standardized quantitative assessment in forensic medicine.

2. Materials and Methods

The methodological framework of this study was specifically designed to transform the conventional qualitative assessment of postmortem pupil size into a standardized quantitative workflow based on the Pupil-to-Iris Ratio (PIR), allowing objective measurement, reproducible classification, and statistical comparison across forensic cases.

2.1. Study Design

This preliminary retrospective observational study was designed to evaluate the forensic applicability of the Pupil-to-Iris Ratio (PIR) as a standardized quantitative index for the objective assessment of postmortem pupillary morphology. The primary objective was to investigate the relationship between PIR and postmortem interval (PMI), while simultaneously evaluating its association with demographic characteristics, clinicopathological variables, causes of death, and postmortem toxicological findings. Given the observational and retrospective design, all analyses relating PIR to cause of death or toxicological exposure were considered hypothesis-generating rather than confirmatory. The study was conducted at the Institute of Legal Medicine, University of Cagliari, on a real-world cohort of consecutive forensic autopsy cases undergoing judicial medicolegal investigation during the study period. Only pre-existing postmortem photographs, forensic records, and toxicological data routinely collected during standard medicolegal practice were included. No additional procedures, examinations, or interventions were performed specifically for research purposes. The manuscript was prepared in accordance with the Strengthening the Reporting of Observational Studies in Epidemiology (STROBE) Statement for obser-

vational studies [39]. The study was conducted in accordance with the ethical principles of the Declaration of Helsinki and the applicable Italian regulatory framework governing judicial postmortem investigations, including Presidential Decree No. 285/1990. Given its retrospective, observational, non-interventional, non-invasive, and exclusively postmortem nature, the study did not require formal ethical approval. Nevertheless, as an additional safeguard of ethical compliance, the protocol was submitted to the competent Independent Ethics Committee of the University of Cagliari. Following its evaluation, the Committee confirmed that formal ethical approval was not required and issued a nihil obstat to the principal investigator on 16 December 2016; consequently, no ethics approval code was assigned. All deceased individuals underwent medicolegal examination within judicial proceedings authorized by the competent Public Prosecutor's Office. The present study exclusively analyzed pre-existing, irreversibly anonymized photographs and data collected during routine forensic practice, and no additional procedures, examinations, or images were performed or acquired specifically for research purposes. Ocular photographs were acquired during the routine external examination of the body, prior to autopsy, under judicial authorization. Ocular photography forms part of the routine forensic documentation performed during the external examination at our Institution, providing a permanent medicolegal record of ocular findings. Accordingly, the present retrospective study exclusively analyzed photographs obtained during routine forensic practice, and no additional images were acquired specifically for research purposes. As an additional ethical safeguard, informed consent for the use of postmortem data and images for research purposes was requested from the next of kin whenever feasible. All data were irreversibly anonymized before analysis in compliance with the General Data Protection Regulation (GDPR) and applicable national legislation.

2.2. Study Population

The study population consisted of 83 eligible forensic cases, corresponding to 166 eyes available for bilateral analysis, retrospectively selected from 100 consecutive judicial autopsies performed at the Institute of Legal Medicine, University of Cagliari. Seventeen cases were excluded because of advanced decomposition (n = 6), globe collapse (n = 6), or incomplete toxicological and/or anamnestic data (n = 5). The cohort included 65 males (78.3%) and 18 females (21.7%), with a mean age of 51.29 $\pm$ 17.59 years (range, 20–86 years). The mean postmortem interval (PMI) was 63.53 $\pm$ 44.52 h (range, 3–288 h). As this represents the first preliminary investigation specifically designed to evaluate the forensic applicability of the Pupil-to-Iris Ratio (PIR), no formal a priori sample size calculation was performed. Instead, all consecutive cases meeting the predefined eligibility criteria during the study period were included, thereby reflecting the spectrum of cases routinely encountered in forensic practice. Eligibility required the availability of bilateral ocular photographs acquired during the routine external examination of the body prior to autopsy, together with complete demographic information, documented PMI, certified cause of death, and comprehensive postmortem toxicological investigations. Only cases in which both the pupillary margin and the horizontal white-to-white limbal diameter could be clearly identified were considered suitable for quantitative morphometric analysis. Cases were excluded whenever advanced corneal opacity, severe ocular trauma, collapse of the globe, marked decomposition, or other postmortem artefacts prevented reliable identification of the anatomical landmarks required for PIR calculation. Severe ocular trauma was defined as direct traumatic involvement of the globe or anterior ocular structures sufficient to compromise identification of the pupillary margin or horizontal white-to-white diameter. Cranial trauma in the absence of direct ocular involvement was not an exclusion criterion; therefore, subjects classified in the TRAUMA1 cause-of-death group remained

eligible when both eyes were morphometrically assessable. Cases with incomplete demographic, forensic, photographic, or toxicological data were likewise excluded. Subjects with chronic neurological disorders known to affect pupillary function were excluded to minimize baseline neurological confounding. The objective of the present study was to characterize postmortem pupillary morphology in a routine forensic population rather than in patients with pre-existing neurological disease. The study population intentionally included subjects with a broad spectrum of causes of death and toxicological profiles in order to evaluate the performance of PIR under heterogeneous real-world forensic conditions representative of routine medico-legal practice. Whenever available, premortem clinical documentation was reviewed, including medical history, hospital records, medications, and resuscitation procedures potentially affecting pupillary morphology. For the large majority of subjects, particularly those who died in hospital, comprehensive clinical information was available. Although these variables were systematically considered during case review, no statistically meaningful association with PIR measurements emerged within the present cohort; therefore, they were not included as independent variables in the final multivariable analyses. A limited number of extra-hospital deaths presented incomplete clinical information, reflecting the inherent characteristics of retrospective forensic casework. Postmortem toxicological investigations were performed on peripheral blood and urine samples according to current international recommendations for forensic toxicological investigations and the routine protocols of the Institute of Legal Medicine, using validated analytical methods routinely employed in the forensic toxicology laboratory. For subgroup analyses, cases were classified as belonging to the TOX group only when the certified cause of death was attributed to acute intoxication following a comprehensive medico-legal assessment integrating autopsy findings, circumstantial information, and postmortem toxicological results. Among the 100 consecutively screened cases, 85 bodies (85.0%) were refrigerated at 4 ± 1 °C before examination. Eyelid position at the initial external examination, before ocular assessment, was documented photographically as closed in 88 cases (88.0%) and open or partially open in 12 cases (12.0%). Among the 83 subjects included in the analytical cohort, 78 (94.0%) were refrigerated before examination and 5 (6.0%) were not refrigerated. Eyelids were closed in 78 included subjects (94.0%) and open or partially open in 5 (6.0%). No manipulation of the ocular globes was performed before image acquisition.

2.3. Image Acquisition

Postmortem ocular photographs were obtained during the routine external examination of the body, prior to autopsy, as part of the standard medicolegal documentation. All images were acquired before any manipulation of the eyeballs or periocular tissues, thereby preserving the original postmortem pupillary morphology. To minimize acquisition variability, all photographs were obtained according to the routine photographic protocol of the Institute of Legal Medicine by trained forensic personnel following standardized forensic documentation procedures. Images were acquired using a Sony ZV-E10 digital mirrorless camera (Sony Corporation, Tokyo, Japan) equipped with a Sony E PZ 16–50 mm F3.5–5.6 OSS lens. Whenever possible, the body was maintained in the supine position and the optical axis of the camera was oriented approximately perpendicular to the ocular surface to minimize perspective distortion. As this was a retrospective observational study, minor variations in illumination, camera-to-subject distance, and image acquisition conditions were unavoidable. The potential influence of image scale and geometric distortion on PIR measurement is addressed in Section 2.4. Image eligibility was assessed according to the criteria reported in Section 2.2. Both eyes were analyzed independently whenever image quality was adequate. No image preprocessing capable of modifying ocular morphology was performed before measurement. Images were analyzed in their

original digital format using the dedicated software-assisted workflow described in the following sections.

The dedicated graphical interface was used to implement the previously described manual photographic PIR measurement procedure. The operator identified the horizontal pupillary margins and the nasal and temporal limbal landmarks on each image. The software calculated the horizontal pupil diameter and horizontal white-to-white diameter in pixels and automatically returned their dimensionless ratio. The interface did not perform automated landmark detection, segmentation, image transformation or estimation of absolute anatomical dimensions.

2.4. Definition of the Pupil-to-Iris Ratio (PIR)

Quantitative assessment of postmortem pupil size from retrospective photographs presents a fundamental methodological challenge. Unlike direct ophthalmological examinations, forensic photographs are generally acquired without a calibration scale positioned on the same anatomical plane as the eye. Consequently, linear measurements obtained from digital images cannot be reliably converted into absolute millimetres because the apparent dimensions of anatomical structures depend on multiple acquisition variables, including camera-to-subject distance, focal length, optical or digital zoom, image resolution, sensor characteristics, image scaling, and perspective. These factors substantially limit the reliability and comparability of absolute pupil diameter measurements obtained from heterogeneous photographic archives [34].

Rather than attempting to estimate the true anatomical pupil diameter in millimetres, the Pupil-to-Iris Ratio (PIR) was adopted as the primary morphometric parameter, providing a standardized, anatomically normalized, and scale-independent descriptor of postmortem pupil size that can be objectively compared across photographs acquired under different imaging conditions.

The PIR was defined as the ratio between the maximum horizontal pupil diameter and the horizontal white-to-white corneal diameter, both measured on the same digital image:

$$PIR = \frac{D_{pupil}}{D_{WTW}}$$

where D_{pupil} represents the maximum horizontal pupil diameter and D_{WTW} the maximum horizontal white-to-white limbal diameter. Since both measurements are expressed in the same unit (pixels), their quotient is dimensionless and therefore independent of the original measurement scale under isotropic scaling conditions. The maximum horizontal pupil diameter was operationally defined as the greatest reproducible horizontal distance between the visible nasal and temporal pupillary margins passing through the geometric centre of the pupil. In eyes showing mild postmortem irregularity of the pupillary contour, measurements were performed along the horizontal meridian providing the greatest reproducible anatomical diameter while avoiding corneal reflections, postmortem artefacts, or obscured pupillary margins. The horizontal white-to-white corneal diameter was selected as the normalization reference because it represents one of the most reproducible biometric parameters of the anterior segment, exhibits limited physiological variability in adults, and remains consistently identifiable in routine forensic photographs [40,41]. Compared to vertical iris measurements, the horizontal white-to-white diameter is less affected by eyelid position, ocular rotation, and postmortem exposure, making it particularly suitable for standardized morphometric analysis.

From a geometric standpoint, the PIR is invariant under isotropic scaling transformations because both the numerator and denominator undergo identical magnification. Consequently, variations related to camera-to-subject distance, focal length, optical or digi-

tal zoom, image resolution, sensor characteristics, and image resizing are mathematically cancelled, eliminating the need for external calibration objects or conversion into absolute millimetres. Nevertheless, the PIR does not compensate for non-perpendicular image acquisition, anisotropic perspective distortion, corneal deformation, or severe postmortem ocular collapse, which remain potential sources of measurement error. PIR measurements were performed using a custom software application (Pupillab2.0) specifically developed for the present study to standardize the complete analytical workflow. After manual identification of the anatomical landmarks defining the horizontal pupil diameter and the corresponding white-to-white corneal diameter, the software automatically calculated the Euclidean distances, computed the PIR, linked each measurement to the corresponding case identifier, eye side, demographic characteristics, postmortem interval, cause-of-death category, toxicological findings, and image reference, and automatically generated a structured database for subsequent statistical analyses. The software was developed in Python 3.12.8 and integrates semi-automated morphometric analysis with standardized quality-control procedures, bilateral eye management, automated database generation, and export of publication-ready datasets for statistical analysis. The original photographs remained completely unmodified throughout the measurement process, and no geometric transformations or pixel alterations were performed before measurement. This workflow minimizes manual transcription errors, ensures complete traceability of every measurement, and improves analytical reproducibility. The complete source code and the scripts used for the statistical analyses are publicly available at https://github.com/nioimatteo-hash/PUPILLAB. (accessed on 8 October 2026) Because the present investigation represents the first methodological study introducing the PIR framework, further software refinement and external multicentre validation are planned. The methodological framework adopted in the present study builds upon the digital photography-based pupil-to-iris measurement method described by Fleischer et al., which demonstrated excellent intra- and inter-rater reliability, with reported ICC values ranging from 0.942 to 0.992 (Table 1, p. 793). Their study also identified a statistically significant quartic relationship between spontaneous pupillary changes and postmortem time; however, this finding did not reveal a reproducible chronological pattern suitable for PMI estimation [34]. The principal methodological innovation of the present work consists of integrating this validated morphometric approach with a dedicated software-assisted workflow specifically developed to standardize measurements, automatically generate the analytical database, minimize transcription errors, and facilitate reproducible quantitative analysis in large retrospective forensic cohorts. The original image measurements were not performed under formal blinding to all case-level information. The interface displayed the case identifier and included fields for the structured recording of demographic, postmortem and toxicological data.

Table 1. Proposed operational classification of the postmortem Pupil-to-Iris Ratio (PIR).

PIR	Classification
PIR $\leq$ 0.200	Extreme miosis
0.200 < PIR $\leq$ 0.275	Miosis
0.275 < PIR < 0.460	Neutral
0.460 $\leq$ PIR < 0.600	Mydriasis
PIR $\geq$ 0.600	Extreme Mydriasis

Accordingly, the present study should be regarded as an exploratory application and operational standardization of the previously published photographic PIR measurement procedure, rather than as an independent validation of its reliability under the operator,

images and acquisition conditions of the present cohort. The previously reported ICC of graphic 0.992 refers exclusively to the observers and image set examined by Fleischer et al. and is cited as evidence concerning the reproducibility of the underlying measurement procedure; it does not represent a reliability estimate obtained from the present cohort or from the dedicated graphical interface.

Operational PIR Classification

The horizontal white-to-white diameter provides a consistently identifiable internal anatomical reference in frontal ocular photographs. Population studies have reported mean adult white-to-white diameters of approximately 11.7 mm, while also demonstrating measurable interindividual variability and differences related to demographic and biometric characteristics [40,41]. In the present method, however, the white-to-white diameter was used exclusively as an internal image denominator. Its reported population mean was not used to convert clinical pupil diameters into PIR thresholds or to infer absolute pupillary dimensions from the photographs.

Pupillary constriction and dilatation are physiologically meaningful manifestations of the balance between parasympathetic and sympathetic control of the iris musculature. However, pupil diameter is not a fixed anatomical quantity: it varies substantially according to illumination, adaptation conditions, age, pharmacological exposure, and the specific examination setting [42–44]. Consequently, the terms miosis, neutral morphology, and mydriasis were retained to provide an anatomically and physiologically intuitive description of progressively smaller or larger pupil dimensions, but not to reproduce clinical categories based on absolute pupil diameter.

Neither clinical ophthalmology nor forensic pathology provides universally accepted quantitative definitions of miosis and mydriasis, and absolute pupil-diameter thresholds vary considerably across sources and illumination conditions. To address this limitation in the retrospective forensic setting, we adopted an operational classification based on predefined PIR thresholds rather than absolute millimetric values. Before inspection or statistical analysis of the present dataset, three primary ranges were established: relative miosis (PIR $\leq$ 0.275), neutral morphology (0.275 < PIR < 0.460), and relative mydriasis (PIR $\geq$ 0.460). Two additional boundaries—PIR $\leq$ 0.200 and PIR $\geq$ 0.600—identified the most pronounced degrees of relative pupillary constriction and dilatation, respectively. These thresholds yielded five mutually exclusive categories: extreme miosis (PIR $\leq$ 0.200), miosis (0.200 < PIR $\leq$ 0.275), neutral morphology (0.275 < PIR < 0.460), mydriasis (0.460 $\leq$ PIR < 0.600), and extreme mydriasis (PIR $\geq$ 0.600). These numerical boundaries were predefined independently of the empirical distribution of the present cohort. They were not derived from the white-to-white values reported in references [40,41], from the pupil diameters discussed in references [42–44], through receiver operating characteristic analysis, or by optimization against cause of death, toxicological findings, or any other study outcome. The cited literature supports the anatomical rationale for using white-to-white diameter as an internal reference and the physiological distinction between pupillary constriction and dilatation, but it does not establish the proposed numerical PIR boundaries as normative thresholds.

Accordingly, the physiological terminology indicates the direction and relative magnitude of pupillary constriction or dilatation, whereas the numerical intervals should be interpreted as proposed operational divisions of the continuous PIR scale rather than as established clinical, diagnostic, physiological, or universal forensic cut-offs. These intervals were applied uniformly throughout the study for descriptive analyses, subgroup comparisons, and graphical representation of pupillary morphology. Independent external validation will be required before they can be regarded as general forensic reference limits.

2.5. Biological Interpretation

The proposed PIR classification provides a standardized operational framework for interpreting postmortem pupillary morphology. The five categories—extreme miosis, miosis, neutral, mydriasis, and extreme mydriasis—represent progressively increasing pupil diameters normalized to the horizontal white-to-white corneal diameter. Rather than defining discrete pathological entities, these categories describe a continuous spectrum of pupillary morphology potentially influenced by multiple interacting factors, including premortem autonomic tone, physiological interindividual variability, pharmacological exposure, chronic neurological disorders, ocular diseases, and postmortem biological changes. Following death, progressive biomechanical alterations involving the iris, cornea, anterior chamber, and intraocular pressure may further contribute to changes in ocular morphology. Consequently, the PIR should be interpreted as a quantitative descriptor of postmortem pupillary morphology rather than as a direct surrogate of the premortem physiological pupil diameter. Importantly, these thresholds should not be interpreted as diagnostic cut-off values but rather as standardized morphometric categories derived from established ophthalmological concepts and adapted for retrospective image-based forensic analysis Figure 1.

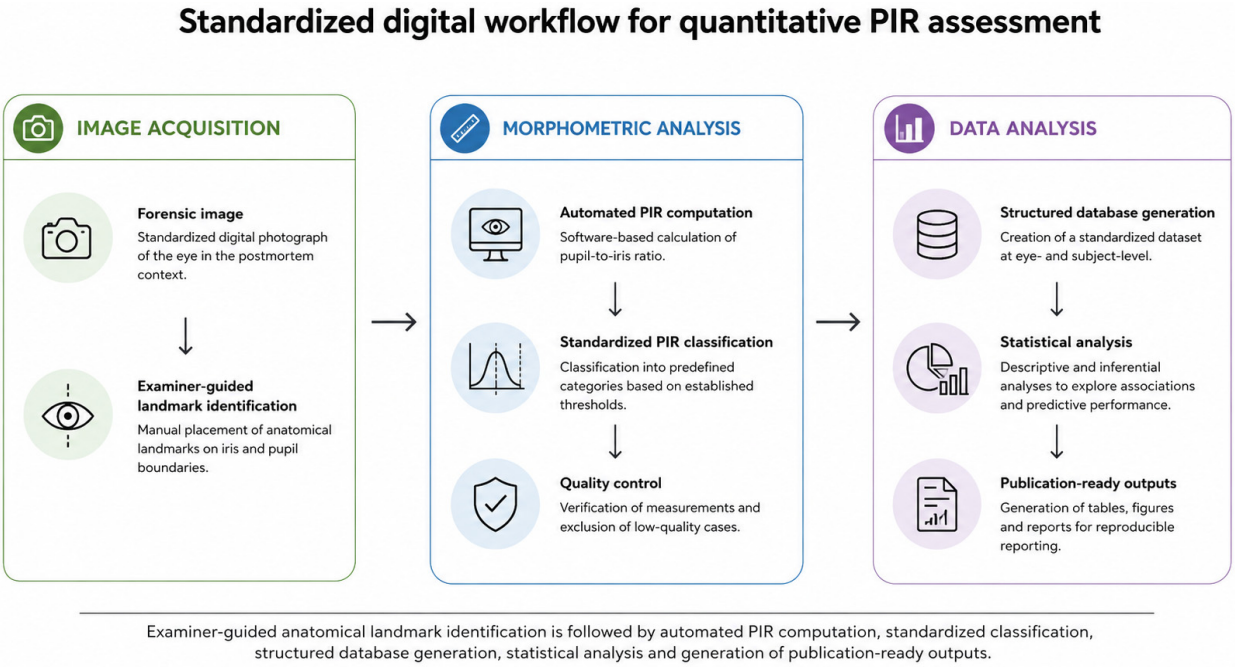


Figure 1. Standardized digital workflow for quantitative postmortem Pupil-to-Iris Ratio (PIR) assessment. The workflow comprises three sequential phases: image acquisition, morphometric analysis, and data analysis. Following acquisition of standardized forensic ocular photographs, the examiner manually identifies the anatomical landmarks required for measurement. The software subsequently performs automated PIR computation, standardized proposed operational PIR classification, structured database generation, statistical analyses, and production of publication-ready outputs. This workflow was specifically designed to improve measurement standardization, reproducibility, traceability, and analytical consistency while maintaining direct examiner supervision during anatomical landmark identification.

2.6. Measurement Procedure

All measurements were performed using the dedicated software described above on the original digital photographs without image preprocessing or geometric modification. Each eye was analyzed independently following a standardized measurement protocol. For every image, the operator first identified the horizontal white-to-white corneal diameter

by selecting the nasal and temporal limbal margins. Subsequently, the maximum horizontal pupil diameter was measured by identifying the greatest reproducible horizontal distance between the visible nasal and temporal pupillary borders passing through the geometric centre of the pupil. Whenever minor postmortem irregularities of the pupillary contour were present, the measurement was performed along the horizontal meridian that best represented the anatomical pupil diameter while avoiding corneal reflections, eyelid interference, or obscured pupillary margins. After landmark identification, the software automatically calculated both Euclidean distances and computed the corresponding Pupil-to-Iris Ratio (PIR). All measurements were immediately stored within a structured database together with the corresponding subject identifier, eye laterality, demographic variables, postmortem interval, cause-of-death category, toxicological findings, and image reference, thereby ensuring complete traceability of every observation throughout the analytical workflow. Image eligibility was assessed according to the criteria reported in Section 2.2. Whenever both eyes fulfilled the quality criteria, bilateral measurements were included in the analysis. Rather than averaging right and left eyes, both observations were retained because interocular asymmetry represented a secondary outcome of interest. The resulting statistical dependence between fellow eyes was subsequently addressed during statistical analysis using subject-level models specifically designed for correlated data. To improve measurement consistency, all images were analyzed using the same standardized workflow and identical operational definitions throughout the study. The measurement procedure and the anatomical landmarks used to calculate the PIR are illustrated in Figure 2.

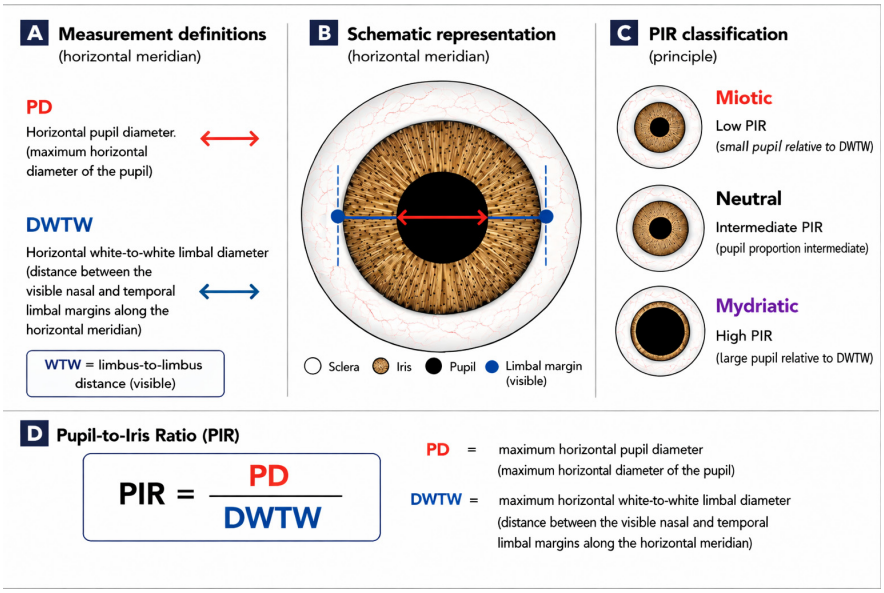


Figure 2. Standardized Pupil-to-Iris Ratio (PIR) Measurement Scheme. (**A**) Definition of the two horizontal measurements used for PIR calculation: maximum horizontal pupil diameter (PD) and horizontal white-to-white diameter (WTW). (**B**) Schematic representation of the measurements along the horizontal meridian. The dashed blue lines indicate the visible nasal and temporal limbal margins used as reference points for DWTW measurement. In routine forensic photographs, the horizontal white-to-white diameter is operationally defined as the distance between the visible nasal and temporal limbal margins, corresponding to the first visible scleral points adjacent to the iris. This visible limbus-to-limbus distance provides a practical and reproducible approximation of the horizontal white-to-white corneal diameter for morphometric analysis. (**C**) Conceptual representation of the standardized PIR categories, illustrating the progressive transition from miotic to neutral and mydriatic morphology as the relative pupil size increases. (**D**) The Pupil-to-Iris Ratio is calculated as PIR = PD/WTW, yielding a dimensionless morphometric parameter suitable for standardized quantitative assessment and comparison of postmortem pupillary morphology.

To assess intra-observer repeatability, a randomly selected subset of 62 eyes (31 subjects) was independently re-measured in a blinded second session. Absolute agreement was quantified using the two-way random-effects single-rater intraclass correlation coefficient [ICC(2, 1)], Bland–Altman 95% limits of agreement, standard error of measurement (SEM), and minimal detectable change (MDC95).

2.7. Study Variables and Case Classification

For each eye, the measurement database generated during the morphometric analysis was integrated with the corresponding demographic, forensic, and toxicological information. Age was recorded in years and analyzed as a continuous variable. Postmortem interval (PMI) was recorded in hours according to the available forensic documentation and analyzed as a continuous variable. For descriptive and comparative analyses, causes of death were classified into predefined categories according to the predominant underlying pathophysiological mechanism. Deaths were grouped as natural (pathological) deaths, toxicological deaths, traumatic deaths involving the central nervous system, and traumatic deaths without direct central nervous system involvement. This classification was designed to distinguish conditions potentially affecting the central autonomic pathways regulating pupillary function from those in which direct neurological involvement was not expected. Toxicological findings were categorized according to the principal pharmacological classes identified during postmortem toxicological investigations. Individual substances were subsequently grouped into predefined toxicological categories to facilitate statistical analyses while preserving the original toxicological information. Because multiple substances could be detected in the same individual, toxicological variables were analyzed both individually and according to their pharmacological class whenever appropriate. Measurements were initially recorded at the eye level, allowing independent morphometric evaluation of each eye. Subsequently, subject-level datasets were automatically generated by the analytical software to permit paired-eye comparisons, assessment of interocular differences, and patient-based statistical analyses. The predefined operational PIR classification (extreme miosis, miosis, neutral, mydriasis, and extreme mydriasis) was applied uniformly to all observations throughout the study according to the standardized framework illustrated in Figure 3.

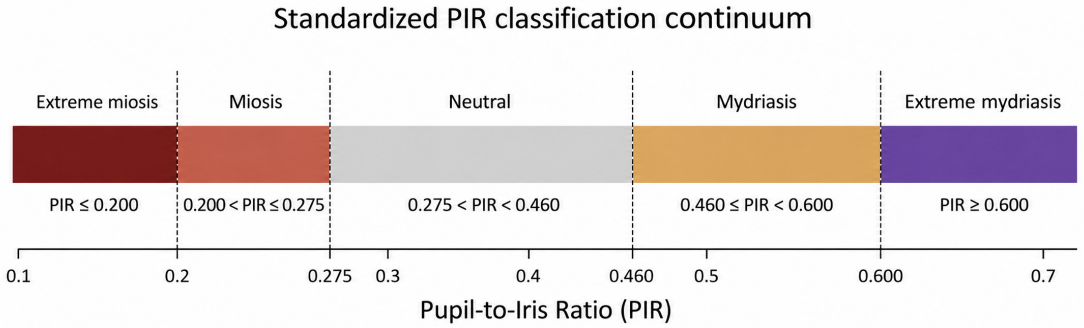


Figure 3. Standardized Pupil-to-Iris Ratio (PIR) Classification Continuum. Graphical representation of the proposed standardized Pupil-to-Iris Ratio (PIR) classification system. The PIR is calculated as the ratio between the maximum horizontal pupil diameter and the horizontal white-to-white corneal diameter, providing a dimensionless measure of postmortem pupillary morphology independent of isotropic image magnification. Based on predefined threshold values, five operational categories were defined: Extreme miosis (PIR $\leq$ 0.200), Miosis (0.200 < PIR $\leq$ 0.275), Neutral morphology (0.275 < PIR < 0.460), Mydriasis (0.460 $\leq$ PIR < 0.600), and Extreme mydriasis (PIR $\geq$ 0.600). The continuum illustrates the progressive transition from maximal pupillary constriction to maximal pupillary dilation and provides the standardized framework used throughout the present study for quantitative morphometric classification.

2.8. Outcome Measures

The primary outcome of the study was the Pupil-to-Iris Ratio (PIR), analyzed both as a continuous morphometric variable and according to the predefined operational categories described above. Secondary outcomes included the distribution of the predefined PIR categories (extreme miosis, miosis, neutral, mydriasis, and extreme mydriasis), interocular asymmetry, and the discriminatory performance of PIR for selected cause-of-death categories and toxicological subgroups. The principal explanatory variables included age, sex, postmortem interval (PMI), cause-of-death category, traumatic mechanism, toxicological findings, and other clinicopathological variables available from the forensic records. Because this was an exploratory methodological study, all associations between PIR and the explanatory variables were considered observational and hypothesis-generating rather than evidence of causal relationships.

2.9. Computer-Assisted Analytical Workflow

The analytical workflow was supported by two custom software applications specifically developed for the present study. The first application was dedicated to image-based morphometric measurements, standardized quality control, and image archiving, generating a structured measurement database directly from forensic photographs. The second application automatically imported the measurement database, generated eye-level and subject-level analytical datasets, constructed derived variables, organized toxicological and forensic information into predefined categories, and prepared the data for statistical analysis. In addition, the software automatically generated graphical visualizations, statistical outputs, and publication-ready reports. The computer-assisted workflow was specifically designed to improve measurement standardization, analytical reproducibility, data traceability, and workflow efficiency while maintaining complete examiner supervision throughout the anatomical landmark identification process. Accordingly, all anatomical landmarks were identified and validated manually by the examiner, whereas all subsequent computational, organizational, and analytical procedures were performed automatically by the software.

2.10. Statistical Analysis

Statistical analyses were performed using the dedicated analytical software developed for the study. Continuous variables were summarized as mean ± standard deviation or median and interquartile range according to data distribution, whereas categorical variables were expressed as absolute frequencies and percentages. Data normality was assessed using the Shapiro–Wilk test.

Because both eyes were available for each subject, eye-level analyses accounted for within-subject clustering using linear mixed-effects regression models with a random intercept for subject. Model assumptions were assessed through residual diagnostics, and the analysis was repeated using logit-transformed PIR as a sensitivity analysis. Categorical outcomes were analyzed using generalized estimating equations (GEEs) with an exchangeable working correlation structure or cluster-robust models, as appropriate, to account for the correlation between fellow eyes. Covariates considered in multivariable analyses included age, sex, PMI, cause-of-death category, and toxicological status. Between-group comparisons were performed using the appropriate parametric or non-parametric statistical tests. Logistic regression models were used to investigate the association between PIR values and toxicological variables, with results reported as odds ratios (ORs) and corresponding 95% confidence intervals (95% CIs). Toxicological analyses were explicitly considered exploratory because of small subgroup sizes, overlapping drug exposures, uncertain timing of intake, and the absence of standardized premortem dose information. For drug-class

analyses, each subject was counted only once within a given pharmacological class, irrespective of the number of individual compounds detected within that class. To address multiplicity in these exploratory toxicological analyses, p values were adjusted within each family of comparisons using the Benjamini–Hochberg false-discovery-rate procedure. Adjusted p values are reported as q values. Diagnostic performance was evaluated by receiver operating characteristic (ROC) curve analysis. Subject-level ROC analyses were performed using bilateral mean PIR for each of the five toxicological outcomes. Raw AUCs were calculated directly from the continuous PIR values. For descriptive presentation of direction-independent separation, a direction-normalized AUC was additionally calculated uniformly as max(AUC, 1 − AUC) for all outcomes [45]. All statistical tests were two-sided, with statistical significance established at $p < 0.05$. For analyses subjected to multiplicity correction, statistical significance was determined using $q < 0.05$.

3. Results

A total of 83 consecutive postmortem subjects (166 eyes) fulfilled the study inclusion criteria and were included in the final analysis. The cohort had a mean age of 51.3 ± 17.6 years and a mean postmortem interval (PMI) of 63.5 ± 44.5 h. The study population included pathological deaths (PAT, n = 40 eyes), toxicological deaths (TOX, n = 44 eyes), cranial traumatic deaths (TRAUMA1, n = 46 eyes), and extracranial traumatic deaths (TRAUMA2, n = 36 eyes). The pathological group included natural deaths due to medical conditions, whereas the toxicological group comprised deaths attributed to acute intoxication. Cranial traumatic deaths included cases with direct traumatic involvement of the central nervous system, while extracranial traumatic deaths comprised traumatic fatalities without direct central nervous system injury. Complete demographic and clinical characteristics are summarized in Table 2.

Table 2. Demographic, postmortem, morphometric, and forensic characteristics of the study population (n = 83 subjects). PIR summary statistics are reported at the subject level using bilateral mean PIR values; eye-level analyses included 166 eyes.

Variable	Value
Subjects	83
Eyes analyzed	166
Age, years	51.3 ± 17.6
PMI, h	63.5 ± 44.5
Mean PIR	0.386
Median PIR (IQR)	0.385 (0.336–0.439)
Interocular asymmetry > 0.10, n (%)	6 (7.2%)
Pathological deaths, n (%)	20 (24.1%)
Toxicological deaths, n (%)	22 (26.5%)
Cranial traumatic deaths, n (%)	23 (27.7%)
Extracranial traumatic deaths, n (%)	18 (21.7%)

3.1. Distribution of Postmortem Pupil-to-Iris Ratio

The eye-level PIR values showed a continuous distribution across the proposed spectrum, ranging from extreme miosis to extreme mydriasis. Application of the standardized PIR classification demonstrated that the Neutral category represented the predominant postmortem pupillary phenotype, accounting for 119 of 166 eyes (71.7%). Mydriasis was observed in 27 eyes (16.3%), whereas miosis was identified in 15 eyes (9.0%). Extreme pupillary morphologies were uncommon, with 2 eyes (1.2%) classified as extreme miosis and 3 eyes (1.8%) as extreme mydriasis, as illustrated by the overall distribution of PIR categories in Figure 4.

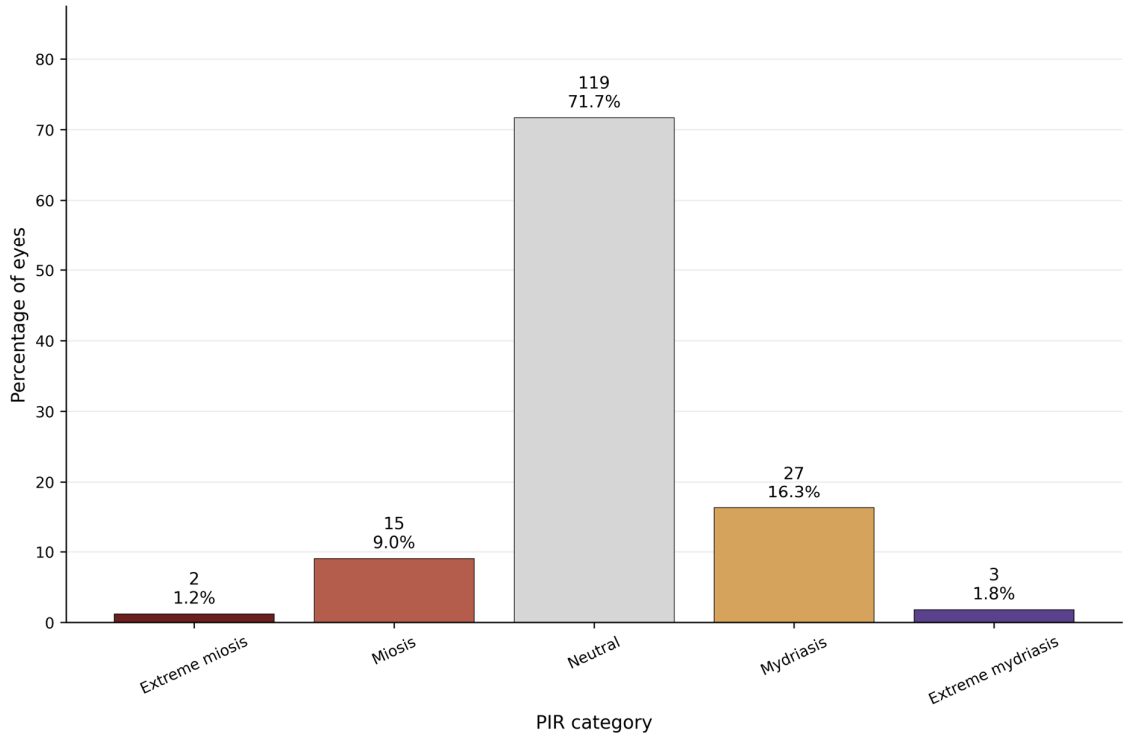


Figure 4. Distribution of Postmortem Pupillary Morphology According to the Standardized PIR Classification. Eye-level distribution of the five predefined Pupil-to-Iris Ratio (PIR) categories in the study population (166 eyes). Each bar represents the proportion of eyes classified as Extreme miosis (PIR $\leq$ 0.200), Miosis (0.200 < PIR $\leq$ 0.275), Neutral morphology (0.275 < PIR < 0.460), Mydriasis (0.460 $\leq$ PIR < 0.600), or Extreme mydriasis (PIR $\geq$ 0.600). Neutral morphology accounted for the majority of examined eyes, whereas extreme categories were uncommon. Absolute frequencies and corresponding percentages are reported above each bar.

3.2. Biological Determinants of Postmortem PIR

3.2.1. Association with Age

A significant inverse association was observed between age and subject-level PIR. Spearman correlation analysis demonstrated a moderate negative correlation ($\rho = -0.352$, $p = 0.001$), indicating progressively lower PIR values with increasing age, as illustrated in Figure 5.

At the eye level, the same trend remained evident across the entire age spectrum irrespective of cause-of-death category. The negative association persisted after accounting for bilateral measurements using mixed-effects regression models, confirming age as the principal biological determinant of PIR within the present cohort. Consistent with the continuous analysis, stratification by predefined age classes demonstrated a progressive shift from predominantly mydriatic morphologies in younger subjects toward neutral and miotic morphologies in older individuals (Supplementary Figure S1). Overall, age represented the strongest physiological variable associated with postmortem pupillary morphology in the present study.

3.2.2. Sex

Sex was not significantly associated with PIR. In the subject-level sensitivity analysis based on bilateral mean PIR, using ordinary least-squares regression with HC3 robust standard errors and adjustment for age and PMI, male sex was not significantly associated with PIR compared to female sex ($\beta = -0.0149$, 95% CI -0.0513 to 0.0216, $p = 0.424$). The corresponding eye-level mixed-effects analysis, which accounted for bilateral measurements through a subject-specific random intercept, is reported separately in Table S1.

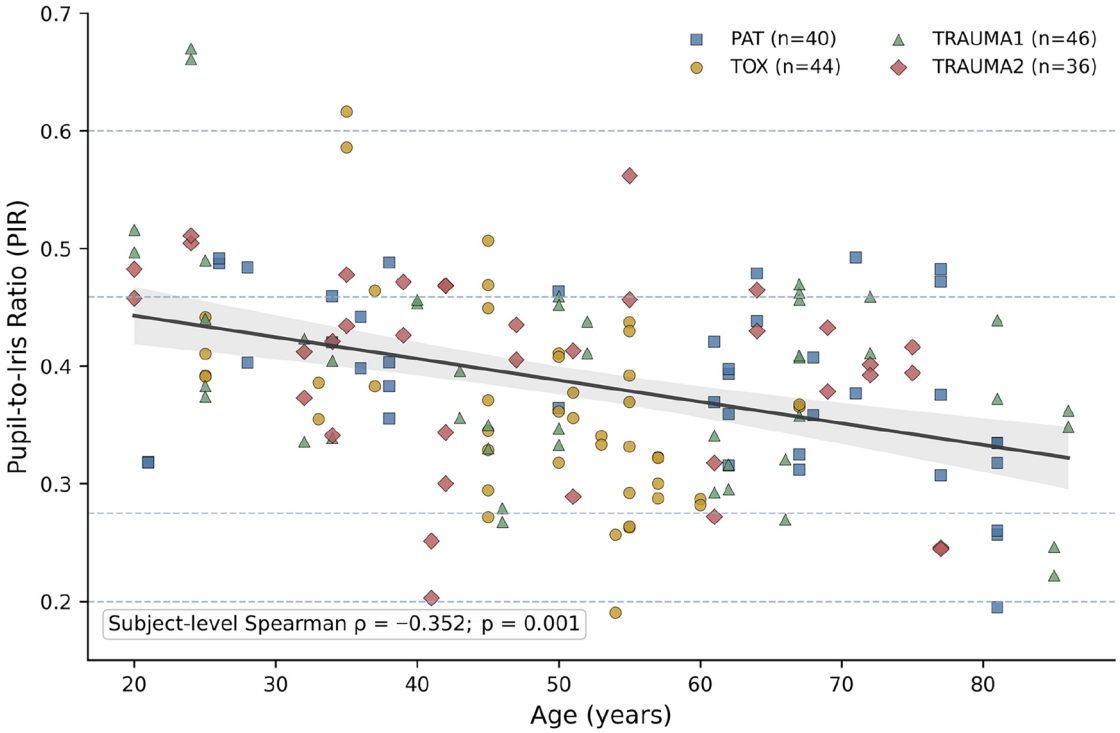


Figure 5. Association between age and postmortem pupil-to-iris ratio (PIR). Scatterplot showing the relationship between age and subject-level bilateral mean PIR in 83 postmortem subjects. Each point represents one subject. The solid line represents the fitted linear trend, and the shaded area indicates the 95% confidence interval. The horizontal dashed lines indicate the predefined PIR thresholds (0.200, 0.275, 0.460, and 0.600) used to delimit the standardized pupillary morphology categories from extreme miosis to extreme mydriasis. Spearman correlation analysis showed a significant inverse association between age and bilateral mean PIR ($\rho = -0.352$, $p = 0.001$).

3.2.3. Association with Postmortem Interval

No significant association was identified between postmortem interval and subject-level PIR. Spearman correlation analysis demonstrated only a weak inverse correlation that did not reach statistical significance ($\rho = -0.169$, $p = 0.128$). Similarly, regression analyses performed after adjustment for the principal covariates did not identify PMI as an independent predictor of PIR values. Across the examined postmortem interval, no consistent trend toward progressive pupillary constriction or dilation was observed.

3.2.4. Bilateral Symmetry

The mean subject-level PIR was 0.386 (median: 0.385; IQR: 0.336–0.439), corresponding to an identical eye-level mean because of the balanced bilateral study design. The conditional ICC from the mixed-effects model was 0.789, indicating substantial within-subject clustering of bilateral measurements. Marked asymmetry, exploratorily defined as an absolute interocular PIR difference greater than 0.10, was observed in only 6 of 83 subjects (7.2%). The residual variance of the final mixed-effects model was 0.001309, corresponding to a residual standard deviation of 0.0362. Because the subject-specific random intercept cancels when the two eye measurements are differenced, the model-implied standard deviation of the interocular difference was $\sqrt{(2\ x\ 0.001309)} = 0.0512$, assuming independent eye-level residuals. Accordingly, the predefined threshold of 0.10 corresponded to approximately 1.95 standard deviations of the model-implied interocular difference. None of the 23 subjects with cranial trauma (TRAUMA1) showed marked asymmetry, compared to 6 of 60 subjects (10.0%) in the remaining study population; this difference was not statistically significant (Fisher's exact test, $p = 0.180$). The threshold was predefined

for descriptive purposes and was not derived from the observed asymmetry distribution. This variance-based calculation provides an internal quantitative anchor but does not validate the threshold as a diagnostic cut-off. Overall, marked postmortem anisocoria was uncommon in the present cohort.

3.3. Postmortem Pupillary Morphology According to Cause of Death

The distribution of postmortem pupillary morphology according to the predefined cause-of-death categories is shown in Figure 6.

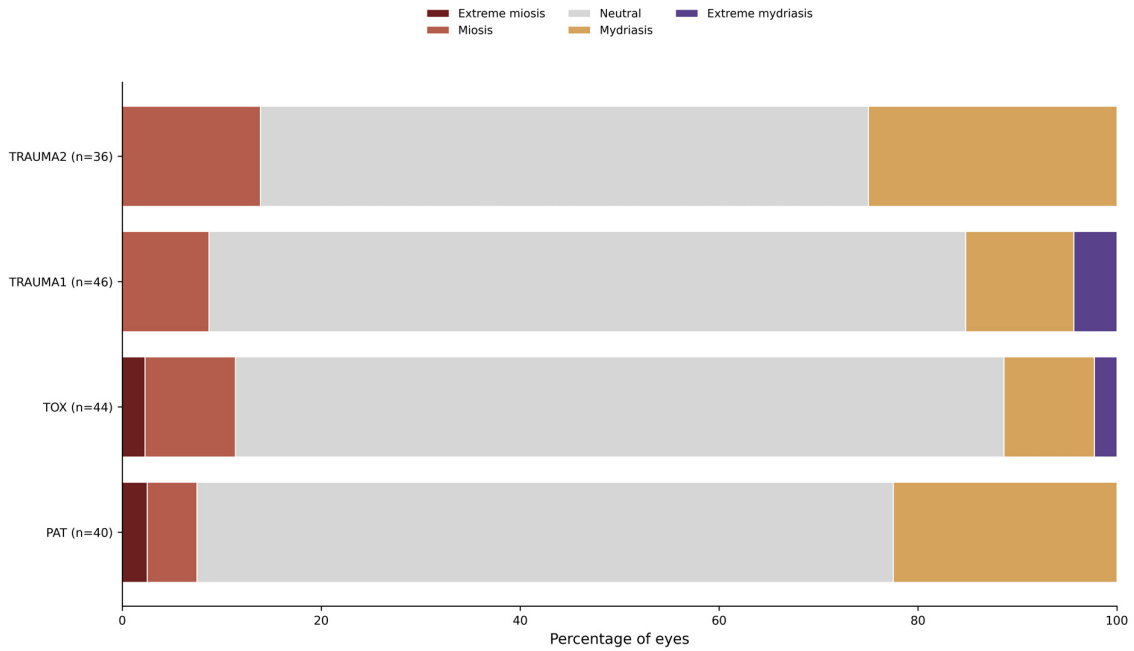


Figure 6. Distribution of Postmortem Pupillary Morphology According to Cause of Death. Distribution of the five standardized PIR categories across the four predefined cause-of-death groups (PAT, TOX, TRAUMA1, and TRAUMA2; n = 166 eyes overall) Horizontal stacked bars represent the percentage of eyes within each cause-of-death category classified as Extreme miosis, Miosis, Neutral, Mydriasis, or Extreme mydriasis. The Neutral category remained the predominant morphological pattern across all cause-of-death groups, although modest differences in the relative distribution of the remaining categories were observed.

The Neutral category remained the predominant pupillary phenotype within each cause-of-death group, accounting for the majority of examined eyes irrespective of the underlying mechanism of death. Stacked category analysis demonstrated only modest variations in the relative proportions of extreme miosis, miosis, neutral morphology, mydriasis, and extreme mydriasis across the four forensic categories. Continuous analysis yielded mean subject-level PIR values of 0.386 $\pm$ 0.069 for pathological deaths (PAT), 0.366 $\pm$ 0.080 for toxicological deaths (TOX), 0.394 $\pm$ 0.090 for cranial traumatic deaths (TRAUMA1), and 0.397 $\pm$ 0.082 for extracranial traumatic deaths (TRAUMA2). No statistically significant difference was observed among the four cause-of-death categories (one-way ANOVA, F = 0.612, p = 0.609), with substantial overlap of individual PIR measurements across all groups. Likewise, the continuous PIR distributions showed broad overlap without evidence of distinct morphometric profiles attributable to a specific cause of death. Multivariable regression analyses adjusting for age and postmortem interval did not identify cause-of-death category as an independent determinant of PIR within the present cohort. The distribution of PIR values across cause-of-death categories is shown in Figure 7.

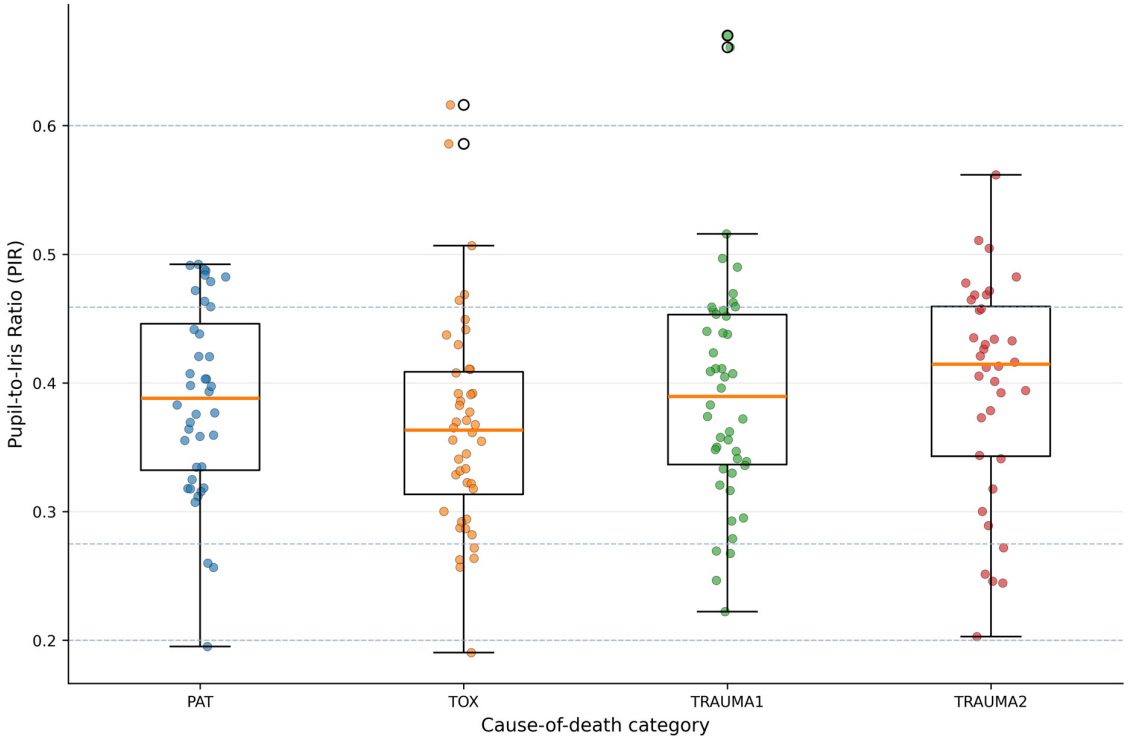


Figure 7. Distribution of Pupil-to-Iris Ratio (PIR) Values According to Cause of Death. Box-and-scatter plot showing the distribution of eye-level Pupil-to-Iris Ratio (PIR) values across the four predefined cause-of-death categories: pathological deaths (PAT), toxicological deaths (TOX), cranial traumatic deaths (TRAUMA1), and extracranial traumatic deaths (TRAUMA2), n = 166 eyes overall. Each point represents a single eye. Boxes indicate the interquartile range (IQR), the horizontal line represents the median, whiskers correspond to 1.5 × IQR, and open circles indicate boxplot outliers beyond 1.5 × IQR from the quartiles. Individual observations are displayed using jittered scatter points. Horizontal dashed lines indicate the predefined PIR thresholds separating Extreme miosis, Miosis, Neutral, Mydriasis, and Extreme mydriasis.

3.4. Association Between PIR and Toxicological Findings

Toxicological analyses were performed to explore possible associations between postmortem pupillary morphology and the presence of psychoactive substances. Overall, the prevalence of Neutral PIR morphology remained high regardless of toxicological status. Exploratory comparisons suggested modest variations in PIR distribution among selected drug classes; however, considerable overlap between exposed and non-exposed subjects was observed for all evaluated substances. Mixed-effects and generalized estimating equation models incorporating age, postmortem interval, and toxicological variables did not identify any toxicological category as an independent predictor of PIR after adjustment for potential confounding factors. Exploratory odds ratio analyses revealed no statistically significant associations between individual drug classes and the predefined PIR categories, with all 95% confidence intervals including the null value. The corresponding forest plot is presented in Supplementary Figure S2. Subject-level ROC analyses based on bilateral mean PIR showed limited discriminatory performance. Raw AUCs were 0.394, 0.406, 0.415, 0.447, and 0.398 for any substance, opioids, cocaine, ethanol, and benzodiazepines, respectively. Direction-normalized AUCs, defined uniformly as max(AUC, 1 − AUC), ranged from 0.553 to 0.606. Subgroup sizes and individual AUC estimates with their 95% confidence intervals are reported in Supplementary Figure S3. Ketamine was not interpreted because only one subject was positive. Six subjects were classified as benzodiazepine-positive. Seven individual benzodiazepine detections were recorded because one subject was positive for both alprazolam and diazepam; pharmacological-class exposure was defined at the

subject level as the detection of at least one benzodiazepine. After Benjamini–Hochberg correction within each family of comparisons, none of the toxicological analyses remained statistically significant.

3.5. Multivariable Analysis

In the primary multivariable linear mixed-effects model including 166 eyes from 83 subjects, increasing age was independently associated with lower continuous PIR ($\beta = -0.00194$ per year; SE = 0.000497; 95% CI, −0.00291 to −0.000964; $p < 0.001$). PMI was not significantly associated with PIR ($\beta = 0.000016$ per hour; 95% CI, −0.000384 to 0.000416; $p = 0.939$). No statistically significant independent associations were observed for sex, laterality, or cause-of-death category. The subject-specific random-intercept variance was 0.00491, the residual variance was 0.00131, and the conditional ICC was 0.789. Complete estimates for all fixed effects and variance components of the primary mixed-effects model are reported in Supplementary Table S1. Age- and PMI-adjusted substance-specific models are presented in Supplementary Table S2; none of the investigated substances remained significantly associated with PIR after Benjamini–Hochberg correction. Model diagnostics, alternative specifications, and sensitivity analyses are reported in Supplementary Table S3. Residual diagnostics for the primary linear mixed-effects model showed no evidence of departure from normality or heteroscedasticity (Shapiro–Wilk W = 0.996, $p = 0.918$; Breusch–Pagan LM = 7.379, $p = 0.391$; Table S3). Analyses based on logit-transformed PIR and subject-level bilateral mean PIR confirmed the inverse association between age and PIR and found no significant linear association with PMI, although sensitivity analyses indicated evidence of a non-linear relationship. Additional GEE analyses of operational pupillary categories according to toxicological status and cause of death are reported in Supplementary Tables S4 and S5, respectively. Substance-specific GEE models and analyses of interocular asymmetry are presented in Supplementary Tables S6 and S7. Owing to small subgroup sizes and sparse outcomes, these additional analyses should be interpreted as exploratory.

3.6. Intra-Observer Repeatability Analysis

A randomly selected subset of 62 eyes from 31 subjects was re-measured by the same trained observer using the same application and anatomical landmark definitions, without access to the original measurements. Intra-observer absolute agreement was excellent (ICC(2, 1) = 0.919; 95% CI approximately 0.87–0.96). The mean difference between the repeated measurements was +0.0074, with 95% limits of agreement ranging from −0.050 to +0.065. The paired t-test did not reach statistical significance (t = 1.98, df = 61, $p = 0.052$). The standard error of measurement was 0.021, corresponding to a minimal detectable change at the 95% confidence level of 0.058 on the PIR scale. Five eyes showed an absolute difference greater than 0.05. In a sensitivity analysis excluding these observations, the ICC increased to 0.963 and the mean difference decreased to +0.0012 ($p = 0.656$). Overall, these findings indicate excellent intra-observer repeatability, limited measurement variability, and no statistically significant systematic bias between the two measurement sessions.

4. Discussion

For more than a century, postmortem pupillary morphology has been described using qualitative terms such as miotic, mid-positioned, or mydriatic. Although these descriptors are routinely employed during forensic external examination, they have never been supported by universally accepted quantitative definitions, and their interpretation has therefore remained largely subjective. Consequently, the postmortem pupil has become one of the few routinely documented forensic findings that has not undergone the transition

from descriptive observation to standardized morphometric measurement despite the increasing incorporation of digital imaging, quantitative biometrics, and objective ocular measurements into contemporary forensic ophthalmology [34–38,46,47].

The principal contribution of the present study is therefore methodological. Rather than proposing the pupil as a novel marker of postmortem interval, cause of death, or toxicological exposure, we establish a standardized quantitative framework for the assessment of postmortem pupillary morphology. By expressing pupil size as a dimensionless Pupil-to-Iris Ratio (PIR) and introducing predefined operational thresholds for miosis, neutral morphology, and mydriasis, conventional qualitative observations are transformed into objective morphometric phenotypes that can be measured, reproduced, and compared across observers, institutions, imaging systems, and future studies.

This distinction is fundamental, because biological interpretation requires objective definition of the phenomenon before its determinants can be meaningfully explored. The proposed quantitative categories provide the operational boundaries and common morphometric language previously lacking for postmortem miosis and mydriasis. Within the investigated cohort, neutral morphology represented the predominant phenotype, whereas miotic and mydriatic configurations occurred less frequently. Importantly, this distribution should not be interpreted as defining a universal postmortem pupil, but rather as the quantitative characterization of the present forensic population, providing a standardized reference against which future studies can be compared. The subsequent question is whether postmortem pupillary morphology reflects identifiable biological determinants. Among all investigated variables, age was the only factor consistently associated with PIR after adjustment for potential confounders and within-subject correlation. This finding is biologically plausible and agrees with the well-established age-related reduction in physiological pupil size observed in living individuals [5,6]. Senile miosis has been attributed to structural remodelling of the iris, reduced dilator muscle function, age-related changes in autonomic innervation, and alterations of iris connective tissue. More recent studies further indicate that pupil size is influenced by additional anatomical factors, including refractive status, axial length, anterior-segment configuration, and overall ocular biometry [48,49]. The persistence of this association after death suggests that postmortem pupillary morphology retains measurable characteristics of the premortem ocular phenotype. Nevertheless, the postmortem pupil should not be regarded as a simple reproduction of its final physiological state. Rather, the measured PIR most likely represents the endpoint of a dynamic interaction between individual anatomical characteristics and the agonal and postmortem processes affecting the eye. This interpretation is reinforced by the remarkable bilateral symmetry observed in the present study. Fellow eyes share virtually all relevant biological determinants—including age, sex, systemic disease, pharmacological exposure, cause of death, and environmental conditions—and demonstrated a high degree of morphometric concordance. Accordingly, the statistical analyses appropriately accounted for the non-independence of paired eyes using generalized estimating equations, mixed-effects models, and cluster-robust approaches, thereby avoiding inflation of statistical significance. In contrast, no independent linear or monotonic association was identified between PIR and postmortem interval, although sensitivity analyses suggested a non-linear relationship. This finding does not establish a sufficiently consistent temporal pattern to support the use of PIR for PMI estimation. Rather than indicating morphological stability after death, this finding likely reflects the complexity of postmortem ocular transformation. Unlike variables that evolve through a predominantly monotonic process, postmortem pupillary morphology represents the combined expression of multiple biological phenomena that evolve simultaneously and at different rates. Consequently, the absence of a simple chronological relationship with PMI appears biologically plausible rather than unexpected.

The lack of a direct relationship between PIR and PMI does not imply that the postmortem eye remains unchanged. Instead, it highlights that pupillary morphology is influenced by progressive alterations involving multiple ocular structures. Corneal dehydration, disruption of the tear film, reduction in intraocular pressure, loss of vitreous volume, changes in anterior chamber configuration, and modifications of globe geometry have all been documented during the postmortem interval [35–37,46,50,51]. Because these processes evolve at different rates, their combined effects are unlikely to generate a simple linear change in a single morphometric parameter. Loss of ocular turgor deserves particular consideration. Progressive reduction in intraocular pressure modifies the mechanical equilibrium of the globe and may influence corneal curvature, anterior chamber depth, axial length, and overall ocular geometry [46,51]. Although expressing pupil size as a dimensionless ratio substantially reduces variability related to image magnification, it cannot completely compensate for asymmetric globe deformation, non-perpendicular image acquisition, eyelid pressure, or perspective artefacts. Future prospective studies combining PIR assessment with anterior-segment OCT, Scheimpflug imaging, and direct intraocular pressure measurements could clarify the contribution of these biomechanical factors. Another unresolved issue concerns iris rigour mortis. Unlike skeletal muscle, the chronology and functional consequences of postmortem stiffening of the sphincter and dilator pupillae remain poorly characterized. Nevertheless, experimental biomechanical studies demonstrate that the iris behaves as a mechanically complex tissue whose deformation depends on stromal stiffness, thickness, permeability, and geometry [49,52]. Supravital responses are not unique to the iris: early postmortem skeletal-muscle excitability also persists for a limited period and may be influenced by intrinsic biological factors, further illustrating the heterogeneous and tissue-dependent nature of residual postmortem reactivity [53]. Together, these observations suggest that postmortem pupillary morphology is influenced not only by the premortem autonomic state but also by the evolving biomechanical properties of the iris itself. Optical factors may further influence morphometric measurements. Progressive tear-film disruption, epithelial dehydration, and corneal irregularity alter visualization of anatomical landmarks during the postmortem period [35–37,46]. In living eyes, en-face OCT has also demonstrated that the precorneal tear film is an optically dynamic structure whose configuration can vary during visual fixation, highlighting its potential influence on ocular imaging and landmark definition [54]. The horizontal white-to-white diameter was therefore selected as the normalization reference because of its excellent visibility and relatively limited physiological variability [40,41]. Nevertheless, WTW measurements remain influenced by ocular biometry and may vary among imaging systems [55]. Consequently, although PIR substantially improves standardization, external validation across different acquisition protocols remains essential before universal threshold values can be recommended. Taken together, these observations emphasize that the proposed PIR classification is not intended to simplify the biological complexity of the postmortem eye. Rather, it enables that complexity to be investigated objectively. The toxicological analyses illustrate the distinction between biological plausibility and forensic applicability. In living individuals, opioids typically induce miosis, whereas sympathomimetic stimulants produce mydriasis; cannabis, benzodiazepines, ketamine, and several other substances may also influence pupillary size or dynamics, although their effects vary according to dose, tolerance, concomitant medications, and environmental conditions [18–25,56]. Consequently, it is biologically reasonable to hypothesize that toxicological exposure could influence postmortem pupillary morphology. However, the postmortem pupil represents the endpoint of a complex sequence of events extending from drug administration to death and continuing throughout the early postmortem period. Drug redistribution, chronic tolerance, agonal hypoxia, metabolic disturbances,

cerebral injury, therapeutic interventions, and postmortem tissue changes may all modify or obscure premortem pharmacological effects. Therefore, the absence of reproducible associations between PIR and specific toxicological categories should not be interpreted as evidence that these substances exert no biological influence on the iris, but rather that a single static postmortem morphometric measurement cannot reliably reconstruct highly dynamic premortem pharmacological processes. This interpretation is supported by the statistical analyses. After adjustment for age, postmortem interval, and bilateral clustering, neither mixed-effects models nor generalized estimating equations identified toxicological categories as independent determinants of PIR. Although exploratory odds-ratio analyses suggested possible trends for opioids, benzodiazepines, and ketamine, confidence intervals remained wide and crossed the null value, while ROC analyses demonstrated poor discriminatory performance across all investigated drug classes. Collectively, these findings indicate that PIR should not be considered a surrogate marker of toxicological exposure, but rather a standardized quantitative descriptor of postmortem pupillary morphology suitable for future multimodal forensic investigations. A similar interpretation applies to cause-of-death analyses. Broad forensic categories inevitably encompass biologically heterogeneous mechanisms characterized by different effects on cerebral perfusion, autonomic regulation, agonal duration, and systemic physiology. Mechanical asphyxia represents a particularly illustrative example, as hanging, ligature strangulation, manual strangulation, positional asphyxia, and suffocation differ substantially in their underlying pathophysiology. Experimental studies have documented progressive postmortem ocular alterations following hanging-induced asphyxia [50], although available evidence primarily concerns retinal and scleral changes rather than pupillary morphology. Because mechanically asphyxiated subjects represented only a small proportion of the present cohort, reliable subgroup analyses were not possible, and larger multicentre studies will be required to clarify whether specific mechanisms of death influence standardized PIR measurements. Premortem clinical management represents an additional potential source of variability. Resuscitation procedures, administration of adrenaline, atropine, opioids, sedatives, vasopressors, or neuromuscular blocking agents, restoration of spontaneous circulation, extracorporeal cardiopulmonary resuscitation, and evolving cerebral injury may all modify pupillary characteristics before death. Recent studies demonstrate that quantitative pupillary parameters remain closely related to neurological status following successful resuscitation [57–60]. Consequently, postmortem pupillary morphology should be interpreted as the cumulative result of premortem physiology, disease processes, therapeutic interventions, and postmortem tissue transformation rather than the isolated consequence of a single pathological event. Overall, these findings reinforce the distinction between standardization and biological interpretation as successive stages of scientific investigation. The present study proposes a quantitative classification intended to support adequately powered investigations of the pathological, pharmacological, and environmental determinants of postmortem pupillary morphology. Measurements were performed using predefined anatomical landmarks and a dedicated software-assisted workflow, while statistical analyses appropriately accounted for paired-eye observations through mixed-effects models, generalized estimating equations, and cluster-robust approaches. Because PIR expresses pupil size relative to the visible iris diameter, it minimizes variability related to image magnification and physiological ocular size, allowing objective comparison across routine forensic photographs without the need for specialized ophthalmological instrumentation. However, PIR remains susceptible to correlated errors in pupil and iris delineation. Several limitations should nevertheless be acknowledged. The retrospective single-centre design limited complete standardization of image acquisition and clinical information. Important variables—including intraocular pressure, anterior-segment biometry, corneal

curvature, iris thickness, tear-film integrity, and serial postmortem changes—were not directly measured. Differences in refrigeration and eyelid position may have affected corneal transparency and ocular preservation, potentially influencing case eligibility and measurement reliability. Furthermore, advanced corneal opacity, severe ocular trauma, globe collapse, decomposition, and poor visualization of anatomical landmarks required exclusion because reliable morphometric analysis was no longer possible. The present retrospective study was not originally designed as a dataset-specific reliability investigation. However, to assess measurement repeatability, a randomly selected subset of 62 eyes from 31 subjects was re-measured during a blinded second session by the same trained observer. Intra-observer absolute agreement was excellent (ICC(2, 1) = 0.919), with a small, non-significant mean difference between measurement sessions (+0.0074; $p = 0.052$) and 95% limits of agreement ranging from −0.050 to +0.065. A sensitivity analysis excluding the five eyes with an absolute difference greater than 0.05 confirmed the robustness of the findings, with the ICC increasing to 0.963. These results support the intra-observer repeatability of the implemented measurement procedure. However, inter-observer agreement and generalizability across independent observers, acquisition protocols, and imaging systems remain to be evaluated prospectively. Landmark placement was not performed under formal blinding to all case-level information. Because anatomical landmarks were selected manually, a potential influence of the available information on measurement cannot be completely excluded, although the use of predefined landmarks and automatic calculation of PIR limited operator discretion after landmark selection. Finally, although the proposed thresholds were predefined and informed by the physiological concepts of pupillary constriction and dilatation, they represent operational divisions of the continuous PIR scale rather than clinically or physiologically validated cut-offs. External validation across independent forensic populations, acquisition protocols, and imaging systems remains essential before widespread implementation. Given the limited number of intoxication deaths and the small size of individual cause-of-death and toxicological subgroups, non-significant findings should not be interpreted as evidence of no effect and should be regarded as exploratory. The requirement for bilateral measurability may have preferentially selected better-preserved eyes at longer PMIs, potentially attenuating the observed PIR–PMI association. Accordingly, the absence of a significant association should be interpreted within the selected study cohort. Moreover, PMI is an estimate subject to unquantified uncertainty. Although the quadratic PMI term was statistically significant ($p = 0.010$), the quadratic model significantly improved fit over the linear model (likelihood-ratio test, $p = 0.0098$), and the more flexible spline model also provided a significant improvement in fit (joint likelihood-ratio test, $p = 0.0388$). PIR reduces common scaling effects but may remain affected by parallax, corneal refraction, and optical distortion. Prospective multicentre studies should validate the proposed classification under different environmental conditions, postmortem intervals, causes of death, and toxicological scenarios. Integration with anterior-segment OCT, Scheimpflug tomography, intraocular pressure measurements, and serial postmortem imaging may clarify the respective contributions of ocular biomechanics, tissue dehydration, and globe deformation to postmortem pupillary morphology. At the same time, recent advances in artificial intelligence and ocular image analysis suggest that automated segmentation and machine-learning algorithms may further improve reproducibility and enable quantitative integration of pupillary measurements with other postmortem ocular biomarkers [47,57,61]. Ultimately, by combining a simple dimensionless index with explicit operational criteria, the present study provides a common quantitative language for postmortem pupillary assessment and a methodological basis for future biological, biomechanical, toxicological, and forensic investigations.

5. Conclusions

Building upon the validated Pupil-to-Iris Ratio (PIR) measurement methodology introduced by Fleischer et al., the present study establishes a standardized quantitative framework for the assessment and classification of postmortem pupillary morphology in forensic practice. By integrating a validated morphometric measurement with physiology-based operational definitions of postmortem miosis, neutral morphology, and mydriasis, it provides a simple, reproducible, and objective approach for quantitative pupillary assessment using routine forensic photographs, thereby enabling standardized evaluation across different observers, institutions, and forensic settings. Within this framework, neutral morphology emerged as the predominant postmortem phenotype, while age was the principal independent correlate of PIR. Associations with postmortem interval, cause of death, and toxicological findings require confirmation in larger cohorts. These findings indicate that quantitative postmortem pupillary morphology primarily reflects premortem physiological characteristics that remain measurable after death, while the final pupillary appearance represents the combined effect of anatomical variability, neurological status, pharmacological influences, and early postmortem changes. Rather than redefining the biology of the postmortem pupil, the present study establishes the methodological framework through which that biology can now be objectively investigated. By transforming traditional qualitative descriptions into standardized quantitative phenotypes, it provides the first common morphometric language for postmortem pupillary assessment and lays the methodological foundation for the future development of quantitative postmortem pupillometry.

Supplementary Materials: The following supporting information can be downloaded at https://www.mdpi.com/article/10.3390/forensicsci6040089/s1, Figure S1: Distribution of Standardized Pupil-to-Iris Ratio (PIR) Categories According to Age Class; Figure S2: Forest Plot of Exploratory Associations Between Toxicological Findings and PIR Categories; Figure S3: Exploratory ROC Analysis of PIR According to Toxicological Findings; Table S1: Primary multivariable linear mixed-effects model for eye-level PIR; Table S2: Substance-specific mixed-effects models for eye-level PIR; Table S3: Sensitivity analyses for the association between PIR and covariates; Table S4: GEE models of operational miosis and mydriasis by toxicological group; Table S5: GEE models of operational miosis and mydriasis by cause of death; Table S6: Multivariable substance-specific GEE models; Table S7: Interocular asymmetry models.

Author Contributions: Conceptualization, M.N., P.E.N. and E.d.; methodology, M.N. and P.E.N.; software, M.N.; validation, M.N., P.E.N., E.d., D.A. and A.S.; formal analysis, E.d. and M.N.; investigation, M.N., D.N. and A.C.; resources, P.E.N., E.d. and E.L.; data curation, M.N., D.N. and A.C.; writing—original draft preparation, M.N.; writing—review and editing, P.E.N., E.d., D.A., A.S., D.N., A.C. and E.L.; visualization, M.N.; supervision, P.E.N., E.L., E.d., D.A. and A.S.; project administration, M.N. and P.E.N. All authors have read and agreed to the published version of the manuscript.

Funding: This research received no external funding.

Institutional Review Board Statement: The study was conducted in accordance with the ethical principles of the Declaration of Helsinki, insofar as applicable to research involving deceased individuals. This retrospective, observational, non-interventional study was based exclusively on routinely collected postmortem photographs and forensic records obtained during judicial medicolegal investigations conducted in accordance with applicable Italian legislation (Presidential Decree No. 285/1990). All postmortem examinations were authorized by the competent Public Prosecutor's Office. As an additional safeguard, the study protocol was submitted to the competent Ethics Committee, which determined that formal ethical approval was not required and issued a nihil obstat to the principal investigator on 16 December 2016; consequently, no ethics approval code was assigned.

Informed Consent Statement: Informed consent for the scientific use of postmortem photographs and related forensic data was requested from the legal next of kin whenever feasible, in accordance with institutional practice. All data were irreversibly anonymized before analysis in compliance with the General Data Protection Regulation (GDPR) and applicable national legislation. No identifiable images or personal data are included in this manuscript.

Data Availability Statement: The datasets generated and/or analyzed during the current study are not publicly available because they contain sensitive medicolegal material, including postmortem photographs and forensic records, whose disclosure is restricted by judicial confidentiality, ethical considerations, and applicable data protection legislation. De-identified data may be made available by the corresponding author upon reasonable scientific request, subject to institutional approval and compliance with applicable legal and ethical requirements.

Acknowledgments: The authors gratefully acknowledge the forensic pathologists, pathology residents, and technical staff of the Institute of Legal Medicine, University of Cagliari, whose daily medicolegal practice and systematic acquisition and archiving of forensic documentation provided the foundation for this retrospective study. The measurements were performed using PupilLab (version 2.0), a Python, 3.12.8-based research software developed to standardize manual postmortem pupil-to-iris ratio (PIR) measurement, data recording, and statistical analysis. The source code is publicly available at https://github.com/nioimatteo-hash/PUPILLAB. (accessed on 8 October 2026) The original photographic dataset is not publicly available because it contains sensitive forensic material and is subject to privacy and institutional restrictions. During the preparation of this manuscript, the authors used ChatGPT (GPT-5.6, OpenAI, San Francisco, CA, USA) exclusively to assist with language refinement and editorial revision, in accordance with the journal's policy. All scientific content, data interpretation, methodological decisions, and final manuscript preparation were performed and verified by the authors, who assume full responsibility for the published work.

Conflicts of Interest: The authors declare no conflicts of interest.

Abbreviations

The following abbreviations are used in this manuscript:

AUC	Area Under the Curve
CI	Confidence Interval
GEE	Generalized Estimating Equations
GLMM	Generalized Linear Mixed Model
IQR	Interquartile Range
OR	Odds Ratio
PIR	Pupil-to-Iris Ratio
PMI	Postmortem Interval
ROC	Receiver Operating Characteristic
SD	Standard Deviation

References

1. Spector, R.H. The Pupils. In *Clinical Methods: The History, Physical, and Laboratory Examinations*, 3rd ed; Walker, H.K., Hall, W.D., Hurst, J.W., Eds.; Butterworths: Boston, MA, USA, 1990.
2. McDougal, D.H.; Gamlin, P.D. Autonomic control of the eye. *Compr. Physiol.* **2015**, *5*, 439–473. [CrossRef] [PubMed]
3. Zele, A.J.; Gamlin, P.D. Editorial: The Pupil: Behavior, Anatomy, Physiology and Clinical Biomarkers. *Front. Neurol.* **2020**, *11*, 211. [CrossRef] [PubMed]
4. Wu, F.; Zhao, Y.; Zhang, H. Ocular Autonomic Nervous System: An Update from Anatomy to Physiological Functions. *Vision* **2022**, *6*, 6. [CrossRef] [PubMed]
5. Lazar, R.; Degen, J.; Fiechter, A.-S.; Monticelli, A.; Spitschan, M. Regulation of Pupil Size in Natural Vision across the Human Lifespan. *R. Soc. Open Sci.* **2024**, *11*, 191613. [CrossRef] [PubMed]
6. Nakamura, K.; Bissen-Miyajima, H.; Oki, S.; Onuma, K. Pupil Sizes in Different Japanese Age Groups and the Implications for Intraocular Lens Choice. *J. Cataract Refract. Surg.* **2009**, *35*, 134–138. [CrossRef] [PubMed]

7. Novitskaya, E.S.; Dean, S.J.; Moore, J.E.; Moore, T.C.B.; Nagendran, S.; Sharma, A. Effects of Some Ophthalmic Medications on Pupil Size: A Literature Review. *Can. J. Ophthalmol.* **2009**, *44*, 193–197. [CrossRef] [PubMed]
8. Erdem, U.; Gundogan, F.C.; Dinc, U.A.; Yolcu, U.; Ilhan, A.; Altun, S. Acute Effect of Cigarette Smoking on Pupil Size and Ocular Aberrations: A Pre- and Postsmoking Study. *J. Ophthalmol.* **2015**, *2015*, 625470. [CrossRef] [PubMed]
9. Wardhani, I.K.; Mathôt, S.; Boehler, C.N.; Laeng, B. Effects of Nicotine on Pupil Size and Performance during Multiple-Object Tracking in Non-Nicotine Users. *Int. J. Psychophysiol.* **2020**, *158*, 45–55. [CrossRef] [PubMed]
10. Orum, D.; Kapici, Y.; Markirt, H.G. Alterations in Pupil Diameter Including Photopic, Mesopic, and Scotopic Vision When Not Under the Influence of Alcohol in Alcohol Use Disorder. *Dyna. Med. Theor.* **2025**, *1*, 117–118. [CrossRef]
11. Karavanaki, K.; Davies, A.G.; Hunt, L.P.; Morgan, M.H.; Baum, J.D. Pupil Size in Diabetes. *Arch. Dis. Child.* **1994**, *71*, 511–515. [CrossRef] [PubMed]
12. Cui, L.; Xiao, Y.; Xiang, Z.; Chen, Z.; Yang, C.; Zou, H. Study on the Correlation between Iris Blood Flow, Iris Thickness and Pupil Diameter in the Resting State and after Pharmacological Mydriasis in Patients with Diabetes Mellitus. *BMC Ophthalmol.* **2024**, *24*, 52. [CrossRef] [PubMed]
13. El Ahmadieh, T.Y.; Bedros, N.; Stutzman, S.E.; Nyancho, D.; Venkatachalam, A.M.; MacAllister, M.; Ban, V.S.; Dahdaleh, N.S.; Aiyagari, V.; Figueroa, S.; et al. Automated Pupillometry as a Triage and Assessment Tool in Patients with Traumatic Brain Injury. *World Neurosurg.* **2021**, *145*, e163–e169. [CrossRef] [PubMed]
14. Chen, J.W.; Vakil-Gilani, K.; Williamson, K.L.; Cecil, S. Infrared Pupillometry, the Neurological Pupil Index and Unilateral Pupillary Dilation after Traumatic Brain Injury: Implications for Treatment Paradigms. *SpringerPlus* **2014**, *3*, 548. [CrossRef] [PubMed]
15. Luz Teixeira, T.; Peluso, L.; Banco, P.; Njimi, H.; Abi-Khalil, L.; Chanchay Pillajo, M.; Schuind, S.; Creteur, J.; Bouzat, P.; Taccone, F.S. Early Pupillometry Assessment in Traumatic Brain Injury Patients: A Retrospective Study. *Brain Sci.* **2021**, *11*, 1657. [CrossRef] [PubMed]
16. Nyam, T.-T.E.; Tu, K.-C.; Kuo, Y.-H.; Wang, C.-C.; Liu, C.-F.; Liao, J.-C.; Kuo, C.-L. Age and Pupil Size: Key Predictors of Mortality in Traumatic Brain Injury Patients with GCS 3. *Front. Neurol.* **2025**, *16*, 1536421. [CrossRef] [PubMed]
17. Lieberman, J.D.; Pasquale, M.D.; Garcia, R.; Cipolle, M.D.; Li, P.M.; Wasser, T.E. Use of Admission Glasgow Coma Score, Pupil Size, and Pupil Reactivity to Determine Outcome for Trauma Patients. *J. Trauma* **2003**, *55*, 437–443. [CrossRef] [PubMed]
18. Murray, R.B.; Adler, M.W.; Korczyn, A.D. The Pupillary Effects of Opioids. *Life Sci.* **1983**, *33*, 495–509. [CrossRef] [PubMed]
19. Rollins, M.D.; Feiner, J.R.; Lee, J.M.; Shah, S.; Larson, M.D. Pupillary Effects of High-Dose Opioid Quantified with Infrared Pupillometry. *Anesthesiology* **2014**, *121*, 1037–1044. [CrossRef] [PubMed]
20. Sørensen, V.O.I.; Uhrenholt, S.; Stokholm, J.; Christensen, T.; Bestle, M.H. The Influence of Opioids on Pupil Initial Diameter and Pupillary Dilation Velocity in ICU Patients. *Acta Anaesthesiol. Scand.* **2025**, *69*, e70080. [CrossRef] [PubMed]
21. Rickels, K.L.; Ghaleb, R.; Elhusseiny, A.M.; Chauhan, M.Z.; Toma, J.; Wang, T.; Cheng, D.; Ali, A.; Sallam, A.B. Ocular Manifestations Secondary to Cocaine Abuse. *Surv. Ophthalmol.* **2025**, *70*, 825–832. [CrossRef] [PubMed]
22. Rosse, R.B.; Alim, T.N.; Johri, S.A.K.; Hess, A.L.; Deutsch, S.I. Anxiety and Pupil Reactivity in Cocaine-Dependent Subjects Endorsing Cocaine-Induced Paranoia: Preliminary Report. *Addiction* **1995**, *90*, 981–984. [CrossRef]
23. Campobasso, C.P.; De Micco, F.; Corbi, G.; Keller, T.; Hartung, B.; Daldrup, T.; Monticelli, F. Pupillary Effects in Habitual Cannabis Consumers Quantified with Pupillography. *Forensic Sci. Int.* **2020**, *317*, 110559. [CrossRef] [PubMed]
24. Haider, M.N.; Regan, D.; Hoque, M.; Ali, F.; Ilowitz, A. Effects of Recent Cannabis Consumption on Eye-Tracking and Pupillometry. *Front. Neurosci.* **2024**, *18*, 1358491. [CrossRef] [PubMed]
25. Kuijpers, K.W.K.; Andersson, K.; Winkvist, M.; Niesters, M.; van Velzen, M.; Nyberg, F.; Dahan, A.; Hämäläinen, M.D. Eye Reactions under the Influence of Drugs of Abuse as Measured by Smartphones: A Controlled Clinical Study in Healthy Volunteers. *Front. Neurosci.* **2025**, *18*, 1492246. [CrossRef] [PubMed]
26. Knight, B.; Saukko, P. *Knight's Forensic Pathology*, 4th ed.; CRC Press: Boca Raton, FL, USA, 2016.
27. DiMaio, V.J.M.; Molina, D.K. *DiMaio's Forensic Pathology*, 3rd ed.; CRC Press: Boca Raton, FL, USA, 2022.
28. Marshall, J. The Irritability of the Iris after Death. *Br. Med. J.* **1885**, *1*, 1003–1004.
29. Boyd, A.; Yadav, S.; Swearingen, T.; Kuehlkamp, A.; Trokielewicz, M.; Benjamin, E.; Maciejewicz, P.; Chute, D.; Ross, A.; Flynn, P.; et al. Post-Mortem Iris Recognition—A Survey and Assessment of the State of the Art. *IEEE Access* **2020**, *8*, 136570–136593. [CrossRef]
30. Orrico, M.; Melotti, R.; Mantovani, A.; De Marco, R.; Avesani, B.; De Leo, D. Pupil Pharmacological Reactivity as Method for Assessing Time Since Death Is Fallacious. *Am. J. Forensic Med. Pathol.* **2008**, *29*, 304–308. [CrossRef] [PubMed]
31. Koehler, K.; Sehner, S.; Riemer, M.; Gehl, A.; Raupach, T.; Anders, S. Post-Mortem Chemical Excitability of the Iris Should Not Be Used for Forensic Death Time Diagnosis. *Int. J. Leg. Med.* **2018**, *132*, 1693–1697. [CrossRef] [PubMed]
32. Englisch, C.N.; Alrefai, R.; Martin-Lesan, C.; Seitz, B.; Tschernig, T. Postmortem Sympathomimetic Iris Excitability. *Ann. Anat.* **2024**, *254*, 152240. [CrossRef] [PubMed]

33. Sinpajakpon, P.; Vongpaisarnsin, K. Pupil Sizes of Bodies with Variant Post-Mortem Intervals. *Chulalongkorn Med. J.* **2011**, *55*, 77–87. [CrossRef]
34. Fleischer, L.; Sehner, S.; Gehl, A.; Riemer, M.; Raupach, T.; Anders, S. Measurement of Postmortem Pupil Size: A New Method with Excellent Reliability and Its Application to Pupil Changes in the Early Postmortem Period. *J. Forensic Sci.* **2017**, *62*, 791–795. [CrossRef] [PubMed]
35. Nioi, M.; Napoli, P.E.; Demontis, R.; Locci, E.; Fossarello, M.; D'Aloja, E. Postmortem Ocular Findings in the Optical Coherence Tomography Era: A Proof-of-Concept Study Based on Six Forensic Cases. *Diagnostics* **2021**, *11*, 413. [CrossRef] [PubMed]
36. Nioi, M.; Napoli, P.E.; Demontis, R.; Chighine, A.; De Giorgio, F.; Grassi, S.; Scorcia, V.; Fossarello, M.; D'Aloja, E. The Influence of Eyelid Position and Environmental Conditions on the Corneal Changes in the Early Postmortem Interval: A Prospective Multicentric OCT Study. *Diagnostics* **2022**, *12*, 2169. [CrossRef] [PubMed]
37. Nioi, M.; Napoli, P.E.; Nieddu, D.; Chighine, A.; Fossarello, M.; D'Aloja, E. Creation of an Experimental Animal Model for the Study of Postmortem Dark Scleral Spots. *Forensic Sci.* **2024**, *4*, 487–498. [CrossRef]
38. Bhatt, S.; Sehrawat, J.S.; Gupta, V. A Systematic Review of Iris Biometrics in Forensic Science: Applications and Challenges. *Egypt. J. Forensic Sci.* **2025**, *15*, 12. [CrossRef]
39. von Elm, E.; Altman, D.G.; Egger, M.; Pocock, S.J.; Gøtzsche, P.C.; Vandenbroucke, J.P.; STROBE Initiative. The Strengthening the Reporting of Observational Studies in Epidemiology (STROBE) Statement: Guidelines for Reporting Observational Studies. *PLoS Med.* **2007**, *4*, e296. [CrossRef] [PubMed]
40. Rufer, F.; Schröder, A.; Erb, C. White-to-white corneal diameter: Normal values in healthy humans obtained with the Orbscan II topography system. *Cornea* **2005**, *24*, 259–261. [CrossRef] [PubMed]
41. Hashemi, H.; Khabazkhoob, M.; Yazdani, K.; Mehravaran, S.; Mohammad, K.; Fotouhi, A. White-to-white corneal diameter in the Tehran Eye Study. *Cornea* **2010**, *29*, 9–12. [CrossRef] [PubMed]
42. Hirasawa, K.; Shoji, N.; Kobashi, C.; Yamanashi, A. Effects of mydriasis and miosis on kinetic perimetry findings in normal participants. *Graefes Arch. Clin. Exp. Ophthalmol.* **2015**, *253*, 1353–1361. [CrossRef] [PubMed]
43. Lowenstein, O. Miosis in Argyll Robertson Syndrome and Related Pupillary Disorders. *AMA Arch. Ophthalmol.* **1956**, *55*, 356–370. [CrossRef] [PubMed]
44. Levine, L. Effective Degree of Mydriasis with Phenylephrine and Tropicamide. *Am. J. Optom. Physiol. Opt.* **1976**, *53*, 774–785. [CrossRef]
45. Hanley, J.A.; McNeil, B.J. The Meaning and Use of the Area under a Receiver Operating Characteristic (ROC) Curve. *Radiology* **1982**, *143*, 29–36. [CrossRef] [PubMed]
46. Ang, J.L.; Collis, S.; Dhillon, B.; Cackett, P. The Eye in Forensic Medicine: A Narrative Review. *Asia Pac. J. Ophthalmol.* **2021**, *10*, 486–494. [CrossRef] [PubMed]
47. Trokielewicz, M.; Maciejewicz, P.; Czajka, A. Post-Mortem Iris Biometrics—Field, Applications and Methods. *Forensic Sci. Int.* **2024**, *365*, 112293. [CrossRef] [PubMed]
48. Domdei, N.; Vohnsen, B.; Wahl, S.; Harmening, W.M. Photopic Pupil Size, Foveal Anatomy and Emmetropisation: A Cross-Sectional Study in Adult Eyes. *BMJ Open Ophthalmol.* **2026**, *11*, e002836. [CrossRef] [PubMed]
49. Tan, R.K.Y.; Ng, G.Y.; Tun, T.A.; Braeu, F.A.; Nongpiur, M.E.; Aung, T.; Girard, M.J.A. Iris Morphological and Biomechanical Factors Influencing Angle Closure during Pupil Dilation. *Investig. Ophthalmol. Vis. Sci.* **2024**, *65*, 7. [CrossRef] [PubMed]
50. Dervišević, E.; Lazović-Salčin, E.; Mattar, L.; Zorlak-Čavčić, A.; Bašić, H.; Katica, M.; Kujundžić-Begović, E.; Kapo-Dolan, N.; Sessa, F. Monitoring Changes in the Eyes—The Significance of the Post-Mortem Interval in Asphyxia. *Forensic Sci. Med. Pathol.* **2026**, *22*, 112–120. [CrossRef] [PubMed]
51. Yoshimiya, M.; Noriki, S.; Shimbashi, S.; Uesaka, H.; Hyodoh, H. Postmortem Changes in Porcine Eyes on Computed Tomography Images. *Leg. Med.* **2025**, *73*, 102568. [CrossRef] [PubMed]
52. Whitcomb, J.E.; Amini, R.; Simha, N.K.; Barocas, V.H. Anterior-Posterior Asymmetry in Iris Mechanics Measured by Indentation. *Exp. Eye Res.* **2011**, *93*, 475–481. [CrossRef] [PubMed]
53. Stigter, H.; Kloosterman, J.; Krap, T.; Duijst, W.L.J.M. Intrinsic Factors Influencing the Post-Mortem Mechanical Excitability of Human Skeletal Muscle. *J. Forensic Leg. Med.* **2026**, *117*, 103055. [CrossRef] [PubMed]
54. Napoli, P.E.; Nioi, M.; d'Aloja, E.; Fossarello, M. The Bull's Eye Pattern of the Tear Film in Humans during Visual Fixation on En Face Optical Coherence Tomography. *Sci. Rep.* **2019**, *9*, 1413. [CrossRef] [PubMed]
55. Liao, Y.; Li, P.; Si, L.; Shen, Z.; Yang, S.; Yuan, Z.; Zhang, B.; Xie, L. Agreement of Anterior Segment Parameters Measured by Scheimpflug-Based Scansys and Pentacam HR: A Prospective, Cross-Sectional Comparative Study. *Photodiagnosis Photodyn. Ther.* **2026**, *59*, 105521. [CrossRef] [PubMed]
56. Eijsvogel, P.P.N.M.; Borghans, L.G.J.M.; Prins, S.; Moss, L.; van Kraaij, S.J.W.; van Brummelen, E.; Klaassen, E.; Martin, R.S.; Bautista, E.; Ford, A.P.; et al. Cognitive Effects of Three β-Adrenoceptor-Acting Drugs in Healthy Volunteers and Patients with Parkinson's Disease. *J. Park. Dis.* **2024**, *14*, 1149–1161. [CrossRef] [PubMed]

57. Gurbuzer, N.; Ozkaya, A.L.; Yaylali, E.T.; Tozoglu, E.O.; Baygin, M.; Tasci, B.; Dogan, S.; Tuncer, T. Deep Learning in Forensic Analysis: Optical Coherence Tomography Image Classification in Methamphetamine Detection. *Eng. Appl. Artif. Intell.* **2025**, *159*, 111682. [CrossRef]
58. Beekman, R.; Chakravartty, A.; Nguyen, C.; Perman, S.M.; Wira, C.; Buckley, R.J.J.; Khosla, A.; Miller, P.E.; Greer, D.M.; Gilmore, E.J. The Impact of Pupil Diameter on Assessing Illness Severity and Outcome after Out-of-Hospital Cardiac Arrest in Patients with Unreactive Pupils. *Resuscitation* **2025**, *215*, 110699. [CrossRef] [PubMed]
59. Hamaguchi, T.; Takiguchi, T.; Seki, T.; Tominaga, N.; Nakata, J.; Yamamoto, T.; Tagami, T.; Inoue, A.; Hifumi, T.; Sakamoto, T.; et al. Association between Pupillary Examinations and Prognosis in Patients with Out-of-Hospital Cardiac Arrest Who Underwent Extracorporeal Cardiopulmonary Resuscitation: A Retrospective Multicentre Cohort Study. *Ann. Intensive Care* **2024**, *14*, 35. [CrossRef] [PubMed]
60. Peluso, L.; Oddo, M.; Minini, A.; Citerio, G.; Horn, J.; Di Bernardini, E.; Rundgren, M.; Cariou, A.; Payen, J.-F.; Storm, C.; et al. Neurological Pupil Index and Its Association with Other Prognostic Tools after Cardiac Arrest: A Post Hoc Analysis. *Resuscitation* **2022**, *179*, 259–266. [CrossRef] [PubMed]
61. Zhu, Z.; Wang, Y.; Qi, Z.; Hu, W.; Zhang, X.; Wagner, S.K.; Wang, Y.; Ran, A.R.; Ong, J.; Waisberg, E.; et al. Oculomics: Current Concepts and Evidence. *Prog. Retin. Eye Res.* **2025**, *106*, 101350. [CrossRef] [PubMed]

Disclaimer/Publisher's Note: The statements, opinions and data contained in all publications are solely those of the individual author(s) and contributor(s) and not of MDPI and/or the editor(s). MDPI and/or the editor(s) disclaim responsibility for any injury to people or property resulting from any ideas, methods, instructions or products referred to in the content.